

Superamphiphobic Diblock Copolymer Coatings

Dean Xiong, Guojun Liu,* and Liangzhi Hong

Department of Chemistry, Queen's University, 90 Bader Lane, Kingston, Ontario, Canada K7L 3N6

E. J. Scott Duncan

Department of National Defence, Defence Research and Development Canada Suffield, Box 4000 Stn Main, Medicine Hat, Alberta, Canada T1A 8K6

Supporting Information

ABSTRACT: A new diblock copolymer, poly[3-(triisopropoxy)silyl]propyl methacrylate]-*block*-poly[2-(perfluorooctyl)ethyl methacrylate] (P1 or PIPSMA-*b*-PFOEMA), that bore a fluorinated PFOEMA block and a sol–gel forming PIPSMA block was synthesized by sequential anionic polymerization and was characterized. P1 was then used to coat silica particles. Factors affecting the amount of P1 grafted onto the silica particles by the sol–gel reactions of the PIPSMA block were investigated, and the coating conditions were optimized. At sufficiently high P1-to-silica mass feed ratios, P1 chemically grafted onto silica surfaces to yield a monolayer. While monolayer formation was supported by results of thermogravimetric analyses, dynamic light scattering, atomic force microscopy, and transmission electron microscopy, our X-ray photoelectron spectroscopy study suggested that the monolayer was topped by the PFOEMA block. Depositing these particles onto microscope slides and printing paper yielded rugged silica films. These films were superamphiphobic, and both water and oil droplets (cooking oil, diodomethane, and hexadecane) possessed large contact angles. The films composed of P1-coated silica particles had substantial resistance to etching by aqueous NaOH solution.

KEYWORDS: superamphiphobicity, block copolymer, coatings, sol–gel chemistry



I. INTRODUCTION

On a superhydrophobic surface,¹ water droplets have contact angles larger than 150°. Also, the difference between the advancing and receding contact angles, or contact angle hysteresis, is small so that the droplets readily roll. Examples of superhydrophobic surfaces from nature include lotus leaves² and water-strider legs.³ If a surface repels oil droplets similarly, the surface is superamphiphobic, or self-cleaning.⁴

Many applications are anticipated for superamphiphobic surfaces. For example, skyscrapers with superamphiphobic walls would require minimal to no cleaning.⁵ Ice would not likely form and build up on the superamphiphobic surfaces of power cables, and this should minimize their damage from ice storms.⁶ Also, superamphiphobic coatings on metal surfaces should help reduce metal rusting and corrosion.⁷

One key criterion for superamphiphobicity is the lower surface energy of the coating compared to that of water or oil.^{8–10} Consequently, low-surface-energy fluorinated compounds or polymers are often used to prepare superamphiphobic surfaces. Unfortunately, fluorinated compounds or polymers are expensive. A typical way to prepare a fluorinated surface is to graft a thin layer of a fluorinated compound onto a substrate without changing the bulk composition of the substrate. To modify silica or glass substrates that bear surface silanol groups (Si–OH), for example, one can graft on them a perfluorooctylethyl triethoxysilane

(CF₃(CF₂)₇CH₂CH₂Si(OC₂H₅)₃, FOETREOS) layer.¹¹ FOETREOS grafts onto these substrates because of the triethoxysilane (TREOS) groups. TREOS groups undergo sol–gel reactions, which involve the hydrolysis of the ethoxy groups to yield silanols and then the condensation of different silanol groups to produce siloxane linkages (Si–O–Si).¹² While siloxane formation between different FOETREOS molecules leads to FOETREOS clustering, Si–O–Si formation from silanols derived from FOETREOS and those on silica or glass surfaces results in the chemical grafting of the perfluorooctylethyl (FOE) group. A FOETREOS-modified surface may be superamphiphobic because of the low surface energy provided by the FOE groups. Ideally, superamphiphobicity can be achieved by only grafting one monolayer of FOETREOS onto a substrate.

While FOETREOS-modified silica or glass surfaces have been shown to possess the properties expected of a fluorinated surface,¹¹ we fancied that a grafted FOETREOS monolayer might not be very stable for two reasons. First, each FOE group tail was bonded onto a substrate by no more than three siloxane bonds, and siloxane bonds were known to be labile. For example, they were easily hydrolyzed by water under basic conditions to

Received: June 23, 2011

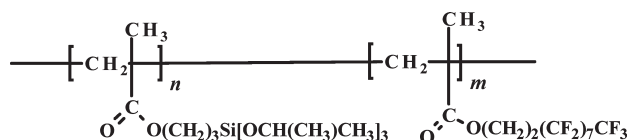
Revised: August 24, 2011

Published: September 06, 2011

yield silanol groups.¹² The fewer the siloxane bonds that held down a FOE group tail, the easier it was for it to detach from a surface. Second, a monolayer consisting of 7 CF₂ and 1 CF₃ units would be very thin and could be easily penetrated by etchants such as a base and water vapor. This would render kinetic feasibility to siloxane hydrolysis.

We further reasoned that this shortcoming could be overcome by a diblock copolymer that incorporated one fluorinated block and one trialkoxysilane-containing block. Analogous to FOETREOS, the trialkoxysilane-bearing block should graft onto a substrate, leaving the low-energy fluorinated block as the exposed top layer. By tuning the lengths of the two blocks independently, one could adjust separately the binding strength with the substrate and the thickness of the fluorinated layer. Because of their inherent thickness and large number of trialkoxysilane units, these diblock copolymer monolayer coatings should be more etchant resistant than monolayers prepared from FOETREOS or other fluorinated small-molecule coupling agents.

On the basis of these considerations, we designed and prepared, in this project, a diblock copolymer poly[3-(triisopropoxysilyl)propyl methacrylate]-*block*-poly[2-(perfluorooctyl)ethyl methacrylate] (PIPSMA-*b*-PFOEMA or P1). P1 was then used to coat silica particles; the factors affecting this coating process were investigated, and the coating process was optimized. Depositing these P1-coated silica particles onto microscope coverslips or printing paper turned these surfaces superamphiphobic. More importantly, the films made of the P1-coated silica particles were shown to be more resistant to NaOH etching than films made of the FOETREOS-coated silica particles, thus verifying our hypothesis.



PIPSMA-*b*-PFOEMA

While the advantages of using P1 or its analogues for superamphiphobic coatings seemed evident, our literature search yielded no reports on diblock copolymers that bore a fluorinated and a cross-linkable block. However, there have been reports on random copolymers made of fluorinated monomers (CH₂=CF₂, CF₂=CF₂, or CF₃CF=CF₂) and cross-linkable monomers [CF₂=CF—(CH₂)₃Si(OR)₃].^{13,14} There have also been many reports on block copolymers containing either fluorinated blocks or trialkoxysilane blocks. A review by Hirao et al.¹⁵ highlighted many fluorine-containing block copolymers. Block copolymers containing trialkoxysilane blocks have been used by the groups of Wiesner¹⁶ and Chen^{17–19} to prepare cross-linked nano-objects.

II. EXPERIMENTAL SECTION

Materials. Tetrahydrofuran (THF) was refluxed with potassium and a small amount of benzophenone until a deep purple color developed, and it was distilled just before use. HCl (4.0 M in dioxane, Aldrich) was diluted with THF to 1.0 or 0.2 M before use. The monomer IPSMA was synthesized following a literature method.²⁰ The monomer FOEMA (97%) and *sec*-butyl lithium (1.4 M in cyclohexane) were purchased from Aldrich. FOEMA was purified by vacuum distillation over calcium hydride before use. Diphenyl ethylene (Aldrich, 97%) was purified by distillation with *sec*-butyl lithium. Tetraethoxysilane (Aldrich,

99.0%), LiCl (Aldrich, 99.99+%), α,α,α -trifluorotoluene (TFT, Acros, 99+%), ammonia (Caledon, 28–30%), FOETREOS (Aldrich, 99.0%), and isopropanol (Fisher, 99.5%) were used as received.

P1 Synthesis. The block copolymer P1 was prepared by the sequential anionic polymerization of IPSMA and FOEMA. The details of P1 preparation are provided in the Supporting Information.

Polymer Characterization. P1 was analyzed at 36 °C by size exclusion chromatography (SEC) using a Waters 515 system equipped with a Waters 2410 differential refractive index detector. The columns used consisted of one Waters μ -Styragel 500 Å column and two Waters Styragel HR 5E columns, and the chloroform eluant flow rate used was 0.4 mL/min. The system was calibrated by monodisperse polystyrene standards.

¹H NMR spectra of P1 were recorded on a Bruker Avance 500 MHz spectrometer. The solvent used was a mixture of TFT-*d*₅ and tetrahydrofuran-*d*₈ (THF-*d*₈) at v/v = 3/1.

Silica Particle Preparation. The silica particles were synthesized following a literature method.^{21,22} Tetraethoxysilane (2.0 g) was dissolved into 21 mL of isopropanol to yield a homogeneous solution before 0.8 mL of an aqueous ammonia solution (28 wt %) was added with vigorous stirring. This mixture was refluxed at 60 °C for 4 h, and the resultant silica particles were settled by centrifugation for 10 min at 3050g. After discarding the supernatant, the particles were redispersed into 10 mL of isopropanol. These particles were settled again by centrifugation, and separated from the supernatant by decantation. This rinsing process was repeated thrice, and the final particles were dried overnight under vacuum.

Coating the Silica Particles. Silica coating by P1 was performed in TFT/THF using HCl as the catalyst. The standard conditions employed a silica-to-P1 mass ratio of 1.00:0.080. The volume fraction of THF in the trifluorotoluene/THF solvent mixture was 9%, and the molar ratio used for IPSMA, H₂O, and HCl was 1/2/1. Furthermore, the grafting reaction was allowed to proceed for 8 h.

In an example run, 5.0 mg of dry silica particles were mixed with 3.0 mL of TFT in a 20 mL vial and ultrasonicated for 60 s to disperse the particles. To this dispersion were then added 0.080 mL of a 5.0-mg/mL P1 solution in THF, 0.14 mL of THF, 0.080 mL of the HCl solution (1.0 M in THF), and 3.0 μ L of H₂O. The mixture was stirred at room temperature for 8 h before it was centrifuged at 3050g for 10 min to settle the particles. After the supernatant was removed, the particles were redispersed in 2.0 mL of TFT and centrifuged again to settle the particles and to remove the supernatant. The particles were rinsed once more to remove the catalyst, byproduct, and any residual polymer that had not grafted. The particles were then vacuum-dried for 2 h in a 100 °C oven.

A similar procedure was used to prepare FOETREOS-coated silica particles. The used silica-to-FOETREOS mass ratio was also 1.00:0.080.

Preparation of a Sol-Gelled P1 Sample. A P1 sample was allowed to undergo the sol-gel reactions under conditions otherwise standard but without silica. After the mixture was allowed to react for 8 h, it was centrifuged at 17,000g for 10 min to settle the product. After the supernatant was removed, the product was redispersed into 2.0 mL of THF and centrifuged. This rinsing process was repeated once again before the product was dried under vacuum to yield a white powder, which should have consisted of nanospheres possessing a PFOEMA corona and sol-gelled PISPMA core.

Thermogravimetric Analyses. Thermogravimetric analyses (TGAs) were performed using a TA Q500 Instrument. A typical measurement involved heating a sample from room temperature to 650 at 10 °C/min.

Diffuse-Reflectance Fourier-Transform Infrared Analyses. Diffuse-reflectance Fourier-transform infrared spectra were obtained for P1, silica particles, and P1-coated silica particles using a Varian 640-IR FT-IR spectrometer. The samples were first dried under vacuum, and then, they were ground with KBr using a mortar and pestle to yield a powder.

X-ray Photoelectron Spectroscopy. X-ray photoelectron spectroscopy (XPS) measurements were performed using a Thermo Instruments Microlab 310F surface analysis system (Hastings, U.K.) under ultrahigh vacuum conditions. The Mg K α X-ray source (1486.6 eV) was operated at a 15 kV anode potential with a 20 mA emission current. Scans were acquired in the fixed analyzer transmission mode with a pass energy of 20 eV and a surface/detector takeoff angle of 75°. All spectra were calibrated to the C 1s line at 285.0 eV, and minor charging effects were observed, which produced a binding energy increase between 1.0 and 2.0 eV. The background of the spectra was subtracted by using a Shirley fitting algorithm and a Powell peak-fitting algorithm.²³

Transmission Electron Microscopy. TFT solutions of silica particles were aero-sprayed onto carbon-coated copper grids and then dried under vacuum at room temperature for 2 h before transmission electron microscopy (TEM) observation. A Hitachi-7000 instrument was operated at 75 kV for obtaining images.

Atomic Force Microscopy. Specimen solutions were aero-sprayed onto silicon wafers. All samples were analyzed by tapping-mode atomic force microscopy (AFM) using a Veeco multimode instrument equipped with a Nanoscope IIIa controller. The Nanosensors NCHR-SPL AFM tips used had a tip radius of ~ 5 nm.

Dynamic Light Scattering. Dynamic light scattering (DLS) measurements were performed at 21 °C using a Brookhaven BI-200 SM instrument equipped with a BI-9000AT digital correlator and a He–Ne laser (632.8 nm). Silica particles were redispersed into methanol, and the P1-coated silica particles were redispersed into TFT for the DLS characterization. The concentrations of the silica particles were approximately 0.5 mg/mL. The samples were centrifuged at 1250g for 15 min for clarification. DLS measurements were performed at 90 °C, and the data were analyzed using the Cumulant method to determine the hydrodynamic diameters (d_h) and the polydispersity index (K_1^2/K_2) values of the samples.²⁴ The TFT refractive index and viscosity used in these calculations were 1.414 and 0.5505 mPa·S, respectively.²⁵

Superamphiphobic Films. P1- or FOETREOS-coated silica particles were redispersed into TFT at a concentration of 2.0 mg/mL. Microscope slide coverslips were coated by casting and evaporating several drops of the silica solution onto the slips. To coat printing paper (Lyreco), the paper was immersed into a P1-coated silica solution for 5 s, withdrawn, and dried under ambient conditions.

Contact Angle Measurements. All contact angles were measured at room temperature (~ 21 °C). The static contact angles were measured using 5 μ L droplets on a KRÜSS K12 tensiometer that was interfaced with image-capturing software. The advancing and receding angles were determined by probing expanding and contracting liquid droplets, respectively. For each sample, the contact angles were measured at 5–10 different positions, and the reported values were the averages of these measurements. The precision of these measurements was better than $\pm 2^\circ$. The liquids that were used for contact angle measurements were Milli-Q water, diiodomethane (>99%, Sigma-Aldrich), vegetable cooking oil (Mazola), and hexadecane (>99%, Sigma-Aldrich).

Robustness of the P1-Coated Silica Films. To demonstrate the better etching resistance of P1-coated silica, coverslips that were coated with films of either P1-coated or FOETREOS-coated silica were first wetted by ethanol by immersing them in ethanol for ~ 3 s. The microscope slides were then withdrawn and quickly immersed into a 1.0 M aqueous NaOH solution. After predesignated times, the films were removed, rinsed with deionized water, and dried under vacuum at 100 °C for 15 min. Then, the contact angles of water droplets on these films were measured.

III. RESULTS AND DISCUSSION

Polymer Synthesis and Characterization. Anionic polymerization was used to prepare P1, because the procedures for

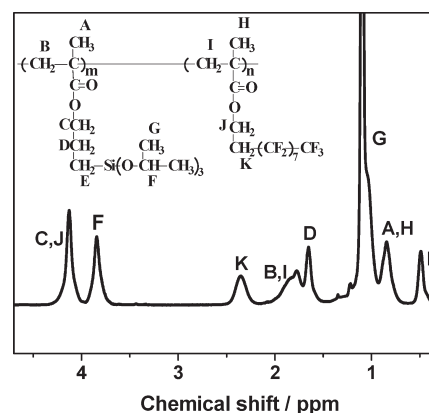


Figure 1. ^1H NMR spectrum of the PIPSPMA-*b*-PFOMA diblock copolymer.

preparing the PIPSPMA²⁰ and PFOEMA²⁶ blocks had been developed previously by Hirao and co-workers. In this proof-of-concept study, only one polymer consisting of 10 IPSMA units and 10 FOEMA units was used. A relatively short FOEMA block was used to ensure the solubility of the resultant diblock copolymer in solvents such as chloroform and deuterated chloroform, which were used for the SEC and ^1H NMR analyses of the polymer.

The polymer was eluted as a single symmetric SEC peak. Based on polystyrene standards, the polydispersity index (M_w/M_n) and number-average molecular weight (M_n) values were 1.16 and 8.6×10^3 g/mol, respectively. Surprisingly, the latter value agreed with the targeted molecular weight.

Figure 1 shows a ^1H NMR spectrum of the diblock copolymer and the peak assignments. The integral ratio of peak E to peak K was 1.0:1.0. This suggested a repeat unit ratio of 1.0:1.0 for PTPOSPMA and PFOEMA, a conclusion fully supported by the integral ratios of the other peaks. By combining the ^1H NMR data with the SEC results, we determined that each of the PTPOSPMA and PFOMA blocks had 10 repeat units.

Silica Particle Synthesis and Characterization. The silica particles used were prepared from triethoxysilane via sol–gel chemistry using a modified Stöber procedure.^{21,22} This process involved the ammonia-catalyzed hydrolysis of the ethoxy groups of triethoxysilane to yield silanol groups and then the condensation of the resultant silanol groups into siloxane bonds. Figures 2a and 3a show a TEM image and an AFM topography image of the silica particles that were prepared. By analyzing over 100 particles, we determined that the particles had an average TEM diameter 325 ± 10 nm. The small (10 nm) standard deviation of the particle diameter suggests a narrow size distribution for the particles.

The TEM images also revealed that the surfaces of the silica particle were not completely smooth but bore craters and bumps. These craters and bumps were also visible in the AFM images. The presence of bumps and craters should not be surprising, because these particles were formed via the incorporation into them of smaller SiO_2 particles formed from TEOS sol–gel chemistry.^{12,27}

A DLS study was also performed on samples of the particles that were dispersed in methanol. The distribution of the hydrodynamic diameters of these particles was plotted in Figure 4a. The average hydrodynamic diameter was 329 nm, which agreed well with the TEM diameter. The DLS polydispersity index of 0.005 confirmed the low polydispersity of the particles.

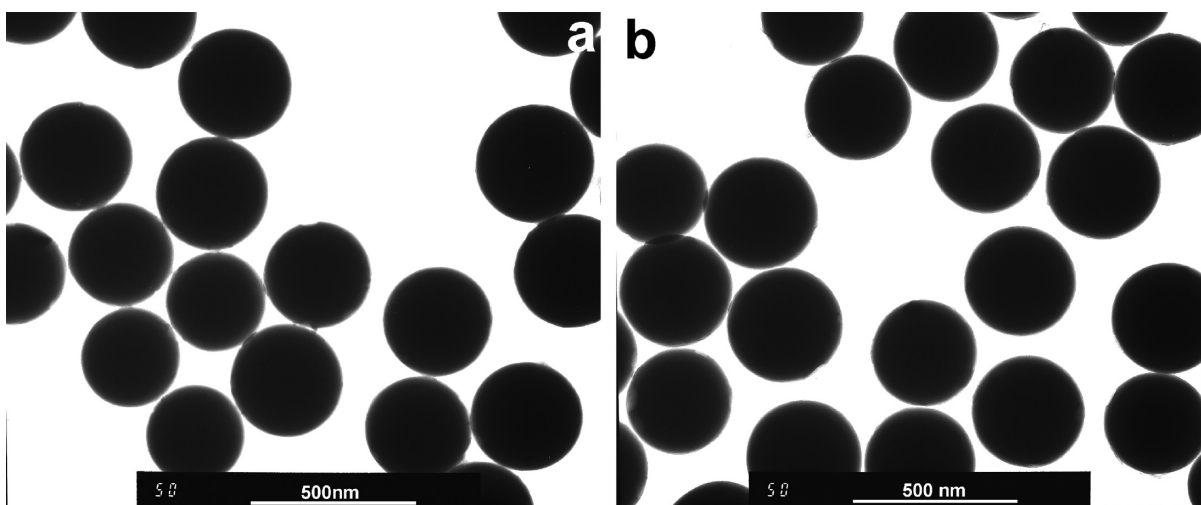


Figure 2. TEM images of the silica particles before (a) and after (b) they were coated by P1 under standard conditions.

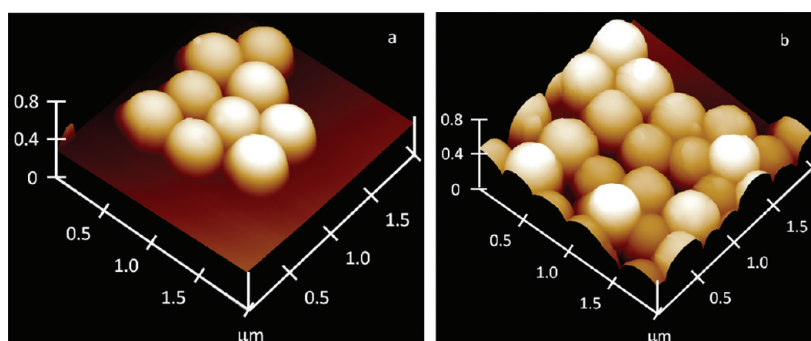


Figure 3. Comparison of AFM topography images of silica particles before (a) and after (b) their coating by P1 at $m_P/m_S = 0.17$ under otherwise standard conditions.

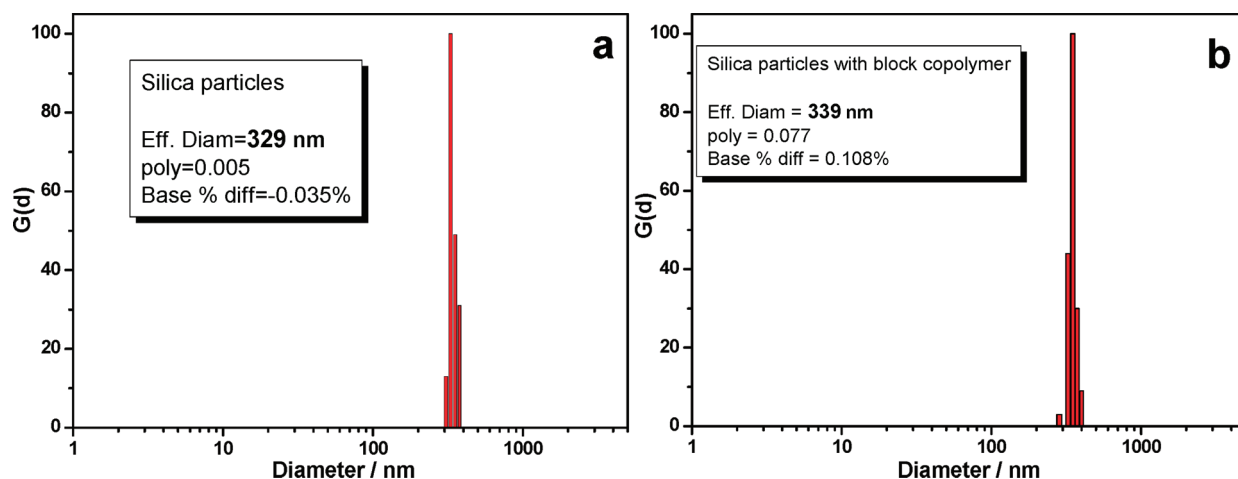


Figure 4. Hydrodynamic diameter distributions of silica particles before (a) and after (b) P1 coating under standard conditions. The solvents used for these two samples were methanol and TFT, respectively.

Silica Coating by P1. Silica was coated by P1 in TFT/THF using HCl as the catalyst.^{11,12} TFT was used to ensure the dispersion of the final particles, which bore a PFOEMA corona. Unless otherwise mentioned, the silica particles were always coated using the standard conditions, which involved performing the grafting reaction at 21 °C

for 8 h in TFT/THF at the THF volume fraction (f_{THF}) of 9.1%. The molar ratio of IPSMA, HCl, and added water was 1/1/2 ($n_{\text{Si}}/n_{\text{HCl}}/n_{\text{H}_2\text{O}}$). The mass ratio used for P1 and SiO_2 (m_P/m_S) was 0.08/1.

Determination of Grafted Polymer Amount by TGA. Figure 5 compares TGA traces of silica, P1-coated silica, and

sol-gelled P1, which was prepared by sol-gelling P1 without silica under conditions otherwise identical to the standard conditions used to graft P1 to silica. When the samples were heated from 200 to 500 °C, the percentile mass residue R_s for silica at 500 °C was 99%. This suggested the thermal stability of silica. Over the same temperature interval, the percentile weight changed for the sol-gelled P1 sample, from 99.0 to 3.79%. Thus, this polymer sample had a percentile mass residue R_p of 3.79/99.0 or 3.82% at 500 °C. Our analyses of 9 P1-coated silica samples yielded a mass residue R_{PS} of $(93.5 \pm 0.3)\%$ at 500 °C.

If we assume that P1 that was grafted onto silica and the sol-gelled P1 had the same TGA characteristics and that the polymer weight fraction in a P1-coated sample was x , the following equation applies:

$$R_s(1 - x) + R_px = R_{PS} \quad (1)$$

For $R_{PS} = (93.5 \pm 0.3)\%$, x was calculated to be $(5.8 \pm 0.3)\%$.

If all of the isopropoxy groups of PIPSMA are hydrolyzed and the resultant silanol groups are fully condensed to form siloxane (Si–O–Si) bonds, the effective chemical formula for a sol-gelled IPSMA unit is $C_7H_{11}O_{3.5}$, where the oxygen number is not an integer because each of the three siloxane oxygen atoms is shared by two Si atoms. Using this effective formula, we calculated that 0.080 g of P1 should yield 0.066 g of grafted polymer. Under the standard silica coating conditions, the P1-to-silica mass ratio used was 0.080/1.00, and the polymer mass fraction in the coated particles should be $0.066/(0.066 + 1.00)$, or 6.2%. This value agreed well with $(5.8 \pm 0.3)\%$, which was

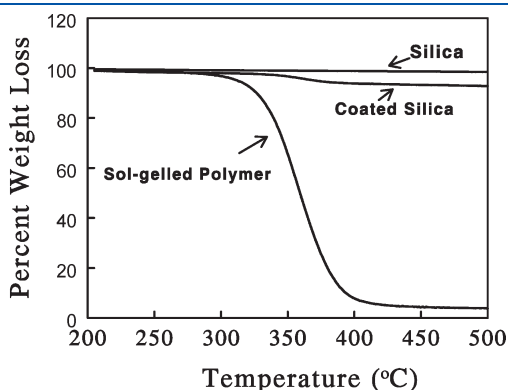


Figure 5. Comparison of TGA curves for silica particles, sol-gelled P1, and silica particles that were coated by P1 under the standard conditions.

determined by TGA, and suggested the validity of the TGA method for quantifying the grafted polymer amount.

The value $(5.8 \pm 0.3)\%$ was slightly lower than 6.2%, probably, because not all of the copolymer was grafted onto the silica surfaces under the standard coating conditions. Rather, some of the copolymer had formed sol-gel micelles and was removed during particle purification.

Factors Affecting P1 Grafting. Using TGA, we determined the grafted polymer amounts Q under different silica coating conditions. Figure 6a shows how Q changed with reaction time, under otherwise standard coating conditions. Q initially increased with reaction time and leveled off after 6 h, suggesting that the grafting reaction required approximately 6 h to complete. Figure 6b shows how Q changed with the molar ratio of HCl to IPSMA (n_{HCl}/n_{Si}), under otherwise standard conditions. Q was low without HCl but was constant after the HCl addition. This behavior was reasonable because not much HCl was required to lower the reaction mixture pH.

Theoretically, one water molecule is required for the formation of one Si–O–Si linkage from two isopropoxysilane groups. Figure 7a suggests that Q changed little with n_{H_2O}/n_{Si} , the molar ratio of water to IPSMA. A probable reason for this is that a trace amount of water either already existed in the solvent or was absorbed from the atmosphere during the grafting reaction.

Figure 7b shows that Q decreased after the THF volume fraction (f_{THF}) in the TFT/THF solvent mixture increased beyond ~9%. The PFOEMA corona was not soluble in THF, but it was in TFT. As f_{THF} increased, the grafted PFOEMA chains should collapse, and hence, the different silica particles should fuse together. The fusion of these particles should slow down the copolymer chain grafting and thus reduce Q .

Figure 8 shows the change in Q as a function of the feed mass ratio of P1 to silica (m_P/m_S). If the added polymer was fully grafted and each IPSMA unit was fully sol-gelled to possess an effective formula of $C_7H_{11}O_{3.5}$, Q should increase linearly with m_P/m_S , as denoted by the dashed line in Figure 8. The calculated and determined Q values agreed with one another at intermediate m_P/m_S values. However, at low m_P/m_S values, Q was lower than the calculated values. Meanwhile, at high m_P/m_S values, Q leveled off and reached a maximum value of ~8.5%.

Q was lower than the calculated values at low m_P/m_S values, probably because the grafted P1 formed islands under these conditions (Scheme 1a). These sol-gelled PIPSMA islands were exposed and might react with moisture during the washing step. This might cause their siloxane bond(s) with the substrate to cleave, and a severed island should readily detach from the silica surface.

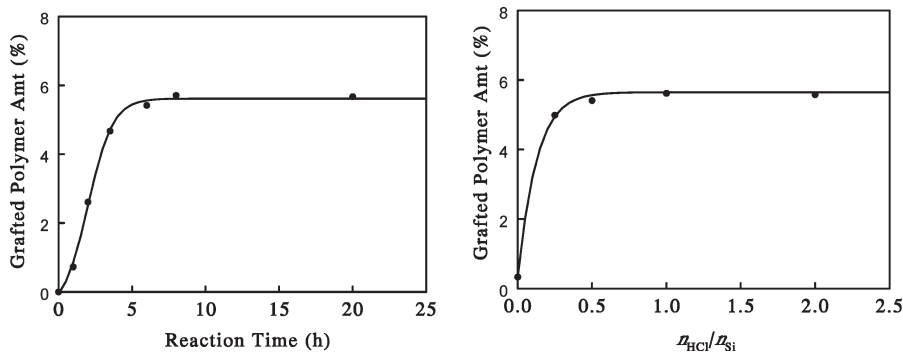


Figure 6. Effect of varying the reaction time (left) and the HCl-to-IPSMA molar ratio, n_{HCl}/n_{Si} , (right) on the amount of P1 that was grafted onto the silica particles under otherwise standard conditions.

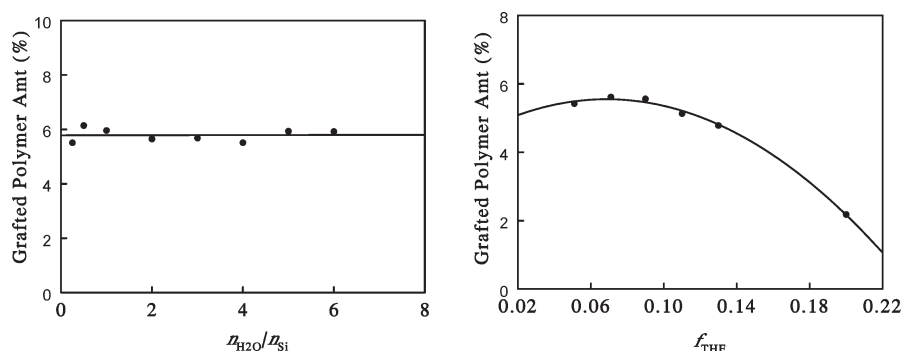


Figure 7. Effect of varying the water-to-Si molar ratio, $n_{\text{H}_2\text{O}}/n_{\text{Si}}$ (left) and the THF volume fraction, f_{THF} (right) on the amount of polymer grafted on silica that was prepared under otherwise standard conditions.

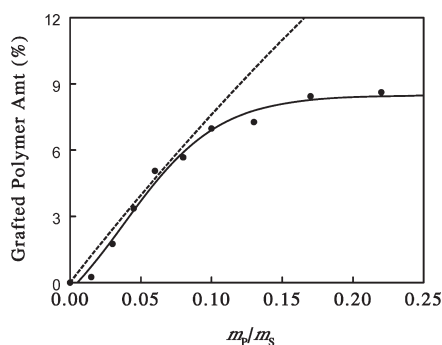


Figure 8. Effect of varying the P1-to-silica mass ratio ($m_{\text{P}}/m_{\text{S}}$), on grafted polymer amount. The grafting experiments were performed under otherwise standard conditions.

Meanwhile, a continuous copolymer monolayer should have formed on the silica surfaces at intermediate and high $m_{\text{P}}/m_{\text{S}}$ values (Scheme 1b). Polymer chain dissociation during the rinsing step from this monolayer should be much more difficult because it would require the cleavage of not only the Si–O–Si bonds between a polymer chain and the silica substrate but also those between this polymer chain and its neighbors. Thus, the predicted and observed Q 's agreed with one another at the intermediate $m_{\text{P}}/m_{\text{S}}$ values. Once a dense monolayer had formed, it rejected the further incorporation of copolymer chains, and thus, Q reached an asymptotic maximum value at high $m_{\text{P}}/m_{\text{S}}$ values.

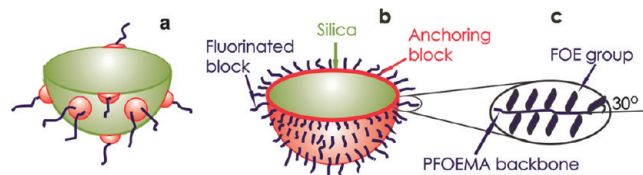
P1 Monolayers on Silica Particles. The density of silica particles (ρ_{S}) prepared from the ammonia-catalyzed reactions of TEOS has been reported to be $\sim 2.2 \text{ g/cm}^3$.²⁷ We assumed that this was the same as the density of the sol-gelled and grafted PIPSMA layer. The density of PFOEMA (ρ_{P}) should be close to 1.85 g/cm^3 , which was calculated for poly[2-(perfluorooctyl)ethyl acrylate] from a group contribution method.²⁸ The density ρ_{P} of the grafted P1 layer including PFOEMA and sol-gelled PIPSMA was thus estimated to be 1.91 g/cm^3 using

$$\frac{1}{\rho_{\text{P}}} = \frac{f_1}{\rho_1} + \frac{(1-f_1)}{\rho_{\text{S}}} \quad (2)$$

Here, f_1 , the mass fraction of the PFOEMA block, was calculated to be 79.6% for P1 with a fully sol-gelled IPSMA block that had an effective formula of $\text{C}_7\text{H}_{11}\text{O}_{3.5}$.

As mentioned previously, the average TEM diameter of the silica spheres (d_{S}) was 325 nm. If the silica particles were assumed to be perfectly spherical, the thickness (h) of a

Scheme 1. Schematic Structures of P1-Grafted Silica Particles Prepared at Low (a) and High (b) P1-to-SiO₂ Mass Feed Ratios and the Packing of the Rodlike Perfluorooctylethyl (FOE) Groups and the PFOEMA Backbone at High P1 Grafting Densities (c)



uniformly grafted P1 layer could be calculated using

$$\left(\frac{d_{\text{S}} + 2h}{d_{\text{S}}} \right)^3 = \frac{Q/\rho_{\text{P}}}{(1-Q)/\rho_{\text{S}}} + 1 \quad (3)$$

At the Q values of 5.8% for coatings prepared under the standard conditions and 8.5% for a saturated layer, the h values were calculated to be 3.8 and 5.6 nm, respectively.

The total number of repeat units was 20 for the P1 chains. Assuming a zigzag conformation for the carbon atoms forming the copolymer's backbone, we calculated a contour length of 5.0 nm for the copolymer backbone. Previous studies suggested that the surfaces of the PFOEMA block should be covered by a liquid crystalline 2-(perfluorooctyl)ethyl layer and the 2-(perfluorooctyl)ethyl group of the terminal FOEMA unit should be directed at a tilt angle of $\sim 30^\circ$ relative to the radial direction of the sphere (Scheme 1c).^{29,30} Thus, a terminal 2-(perfluorooctyl)ethyl unit consisting 10 C–C bonds should add another 1.3 nm to the thickness of a dense monolayer. Thus, the theoretically possible maximum thickness for a grafted P1 layer should be 6.3 nm.

The theoretical maximal thickness of 6.3 nm was comparable with the experimentally determined maximum thickness of 5.6 nm. This suggested that P1 was grafted indeed as a monolayer.

The difference suggests that the polymer chains in the monolayer did not assume the energetically unfavorable, fully stretched configuration. One should further realize that the value 5.6 nm was determined by assuming that the silica particles were perfectly spherical. In reality, the silica particles did bear surface bumps and craters, and a sphere like this should have a surface

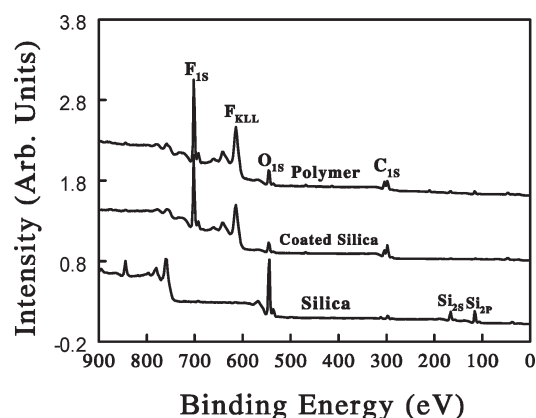


Figure 9. XPS spectra of silica (bottom), P1-coated silica (middle), and P1 (top).

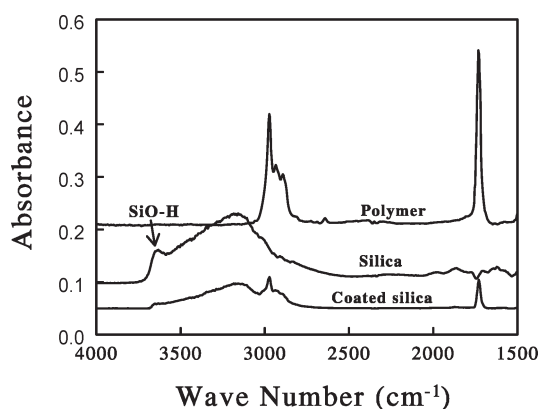


Figure 10. Diffuse reflectance infrared spectra of P1 (top), silica particles (middle), and silica particles that were coated with P1 under the standard conditions (bottom).

area larger than that of an ideal sphere of a similar size. Thus, 5.6 nm represented an overestimate for the thickness of a densely packed P1 layer.

Figure 3 also shows an AFM topography image of a silica sample after its coating by P1 at $m_P/m_S = 19\%$ under otherwise standard conditions. At this m_P/m_S value, the coating should be rather thick, approaching 5.6 nm. After P1 coating, the silica surfaces appeared rather smooth and were free of particles with diameters ~ 10 nm, which should be close to the diameter of the sol-gelled P1 nanoparticles that consisted of a PFOEMA corona and a sol-gelled PIPSMA core. The lack of these small particles confirmed that P1 was grafted as a uniform monolayer.

Figure 2 showed TEM images of silica particles before and after their coating by P1 under the standard conditions. The coated particles appeared to be rather smooth. This again suggested that these particles were uniformly coated by P1. The hydrodynamic diameter of this sample was determined to be 339 nm, which represented a 10 nm increase relative to the uncoated silica particles, or a solvated coating layer thickness of 5 nm. This value was consistent with a dry coating thickness of 3.8 nm.

Compared in Figure 9 are the X-ray photoelectron spectroscopic (XPS) data of silica, P1, and P1-coated silica. Si and O peaks were predominant for the silica sample, as expected. These peaks were present together with F peaks in the P1 sample,

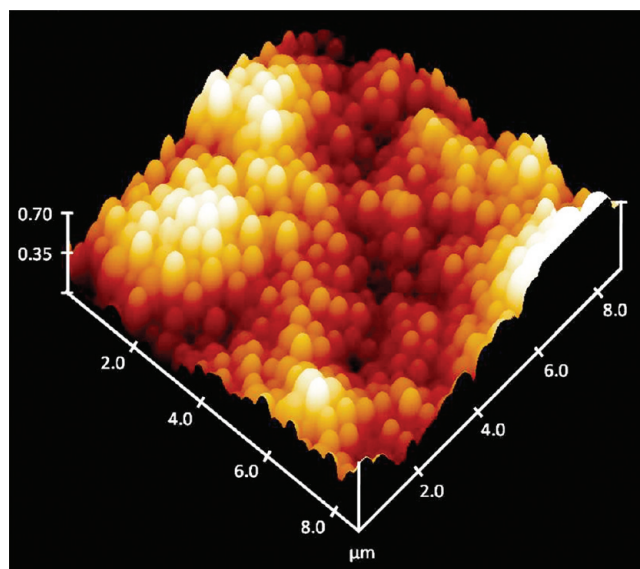


Figure 11. AFM topography image of a fluorinated silica particle film on a glass plate.

because P1 contained Si, O, and F atoms. Interestingly, the intensities of the Si and O peaks decreased relative to the F peaks in the coated silica sample. This suggests that the perfluorooctyl groups constituted the top layer of the coating, even at a moderate coating thickness of 3.8 nm, thus confirming the chain and FOE group unit packing in Scheme 1c.

The chemical grafting of P1 was supported by our diffuse reflectance infrared spectroscopic data. Figure 10 compares infrared absorption spectra of silica, P1, and P1-coated silica. The coated sample bore peaks of both silica and the polymer, as expected. More interestingly, the intensity of the shoulder peak at 3750 cm^{-1} , which was characteristic of silanol units, decreased after the grafting reaction. This suggested that the silanol units of the silica surface had condensed with the sol-gelled PIPSMA block. This also suggested that most of the Si-OH units of the hydrolyzed PIPSMA block were condensed.

Particulate Films. Studies of natural superhydrophobic surfaces, such as lotus leaves^{2,31} and water strider legs,³ have helped to shed light on the essential criteria for superhydrophobicity, in particular, and superamphiphobicity, in general. Aside from a low surface energy, the surfaces should also be rough to render large liquid contact angles.^{4,32,33} An easy way to obtain a rough coating or film is to apply fluorinated nondeformable particles onto a substrate.^{34–41}

P1-coated silica particles dispersed in TFT were cast onto microscope coverslips or glass plates to prepare rough particulate films. Also, particulate films were applied onto printing paper by soaking the paper in a coating solution and subsequently withdrawing the paper from the solution. Figure 11 shows an AFM topography image of a film prepared on a glass plate. Individual coated silica particles could be clearly discerned, and the film was obviously rough.

Despite these apparently crude film preparation protocols, we established that the determined liquid contact angles changed by less than 2° from one particulate film to another for a given sample. The contact angles were, however, readily changed by using silica particles that were coated using different P1-to-silica mass ratios m_P/m_S . Figure 12 shows photographs of water

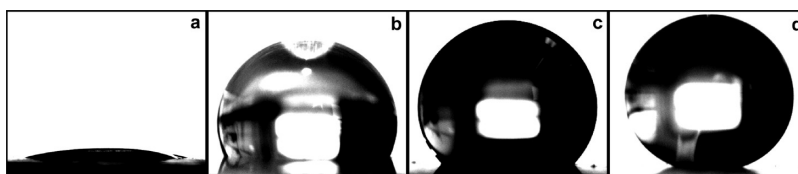


Figure 12. Photographs of water droplets sitting on glass-plate-backed films that were prepared from silica (a) and silica bearing 1.2% (b), 4.8% (c), and 5.8% (d) of grafted polymer.

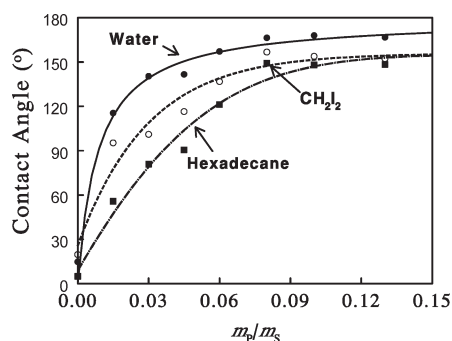


Figure 13. Variation of water (●), CH_2I_2 (○), and hexadecane (■) droplet contact angles as a function of the m_p/m_s used in coating the silica particles. These coatings were applied onto glass microscope slides.

droplets that were dispensed onto films of an uncoated silica particle and films of silica particles that were prepared using the m_p/m_s values of 0.015, 0.045, and 0.08, respectively. As shown in Figure 8, these m_p/m_s values corresponded to Q values of 1.2, 4.2, and 5.8%, respectively. Evidently, the water contact angles increased as Q increased.

Similar trends were observed for the contact angles of methylene iodide and hexadecane droplets on glass-backed films of silica prepared using different m_p/m_s values. Plotted in Figure 13 are the variations in the static contact angles of water, methylene iodide, and hexadecane as a function of m_p/m_s used to coat the silica particles. The contact angles seemed to level off for every liquid when m_p/m_s reached approximately 0.08.

Table 1 shows contact angles for water, methylene iodide, and hexadecane on silica-coated glass slides. The silica particles described in this table were coated under the standard conditions. The static angles were large for all three of the liquids, and the differences between the advancing and receding contact angles, or their hysteresis values, were small. Therefore, these silica films were superamphiphobic. This was a direct result of the fact that the perfluorooctyl groups decorated the silica particle surfaces. The contact angles decreased from water to diiodomethane to hexadecane because the surface tension decreased for these three liquids from 72.8 to 50.8 to 27.5 mN/m, respectively.⁴²

The silica particles seemed to be able to turn any substrate that can be coated superamphiphobic. Figure 14 shows photographs taken immediately after rhodamine-B-impregnated droplets of vegetable cooking oil and water were applied on untreated printing paper and paper that was covered by P1-coated silica. On untreated paper, both water and oil droplets spread and became absorbed by the paper in less than 1 min. On the other hand, no noticeable water or oil sorption was observed after 30 min on treated paper, and the water and oil droplets had equilibrium contact angles of 160 and 153°, respectively.

Table 1. Static, Advancing, and Receding Contact Angles for Water, Diiodomethane, Cooking Oil, and Hexadecane on the Films of Silica Particles Coated by P1 under Standard Conditions

liquid	static contact angle (deg)	advancing contact angle (deg)	receding contact angle (deg)
Silica Films Applied onto Glass Microscope Slides			
water	167 ± 2	170 ± 2	163 ± 2
diiodomethane	157 ± 2	159 ± 2	149 ± 2
hexadecane	149 ± 2	155 ± 2	142 ± 2
Silica Films Applied onto Printing Paper			
water	160 ± 2		
cooking oil	153 ± 2		

Etching Resistance of P1-Coated Silica Films. We started this project on the premise that silica particles coated by P1 should be more resistant to etchant penetration and degradation than those coated by FEOTREOS or other fluorinated small-molecule coupling agents. To verify this, we coated silica with FEOTREOS under the standard conditions using a FEOTREOS-to-silica mass ratio of 0.080/1.00 and applied films of the resultant silica particles onto glass plates. The contact angles of water on these films were also large, at 164°.

However, the films behaved differently when they were soaked in 1.0 M NaOH aqueous solution. After the films of the FEOTREOS-coated silica particles were soaked in 1.0 M NaOH aqueous solution for 3 h, we noticed a film thickness decrease. This was probably caused by the penetration of the sol-gelled FEOTREOS layer on silica by NaOH and then SiO_2 dissolution. After the films were dried, the contact angles of water droplets on the resultant films decreased sharply to below 90°. On the other hand, no physical changes were seen for P1-coated silica films after they were immersed in 1.0 M NaOH aqueous solution between 3 and 5 h. After these films were dried, the water contact angles on these films did not change, confirming the film intactness. More interestingly, soaking glass plates that were covered with P1-coated silica films in a 1.0 M NaOH aqueous solution for 8 h did not disintegrate the film but severed it from the glass substrate. This delamination was most likely caused by the fact that the glass substrate was etched. Thus, the P1-coated silica was much more resistant to NaOH etching than the FEOTREOS-coated silica.

Despite the etching resistance and the outstanding water and oil repellence, one should realize that the films made from P1-coated silica particles could not be mechanically robust because the adhesion among the fluorinated particles and that between the fluorinated particles and the substrate were poor. For robust particulate films, bifunctional particles that bear both surface fluorinated groups and groups that can react with either the

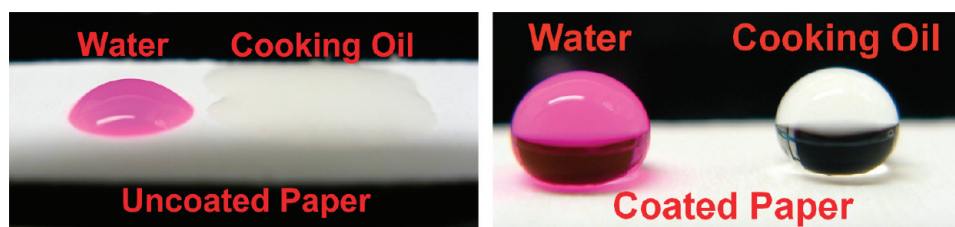


Figure 14. Photograph of cooking oil and water droplets on the surfaces of uncoated (left) and coated (right) printing paper.

substrate or a polymer binder should be used. Robust particulate films have been procured from one type of bifunctional super-amphiphobic particles,⁴³ and a method for bifunctional particle preparation from P1 is currently under development.

IV. CONCLUSIONS

P1 was prepared by the sequential anionic polymerization of IPSMA and FOEMA. It was then used to coat silica particles that were prepared from tetraethoxysilane via sol–gel chemistry and possessed an average diameter of 325 ± 10 nm. The amount, Q , of P1 grafted onto silica particle surfaces could be determined by TGA. This thus allowed us to investigate the effect of varying the reaction time, solvent composition, catalyst HCl amount, water amount, and P1-to-silica mass ratio (m_P/m_S) on Q and to optimize the P1 coating conditions. This systematic study revealed that Q increased initially with m_P/m_S and leveled off at higher m_P/m_S values and therefore suggested P1 monolayer formation at higher m_P/m_S values. Monolayer formation was further supported by our DLS, AFM, and TEM results. An XPS study revealed that the perfluorooctyl groups topped the monolayer, even at a moderate coating thickness of 3.8 nm. Films of P1-coated silica particles were cast onto glass substrates and applied to paper, and the contact angles for water, methylene iodide, and hexadecane were measured. The contact angles varied as a function of m_P/m_S , increasing as the degree of P1 grafting onto the silica particles increased and leveling off for each liquid when m_P/m_S reached approximately 0.08. Static contact angles in the super-repellency regime (150°) were obtained for water and methylene iodide and nearly so for hexadecane (149°), which has a surface tension of 27.5 mN/m. Paper treated with P1-coated silica particles also produced static contact angles in the super-repellency regime for water and cooking oil. The P1-coated silica films were determined to be resistant to NaOH etching. After 3 h of soaking in a 1.0 M NaOH aqueous solution, the water contact angle on the film did not change.

■ ASSOCIATED CONTENT

Supporting Information. Detailed procedure for P1 synthesis. This material is available free of charge via the Internet at <http://pubs.acs.org>.

■ AUTHOR INFORMATION

Corresponding Author

*E-mail: guojun.liu@chem.queensu.ca.

■ ACKNOWLEDGMENT

The Canadian Department of National Defence and NSERC of Canada are thanked for financially sponsoring this research.

Dr. Ian Wyman is thanked for proofreading this manuscript. G.L. thanks the Canada Research Chairs program for a Tier I Canada Research Chair Position in Materials Science.

■ REFERENCES

- (1) Wang, S.; Jiang, L. *Adv. Mater.* **2007**, *19*, 3423–3424.
- (2) Solga, A.; Cerman, Z.; Striffler, B. F.; Spaeth, M.; Barthlott, W. *Bioinspiration Biomimetics* **2007**, *2*, S126–S134.
- (3) Gao, X. F.; Jiang, L. *Nature* **2004**, *432*, 36–36.
- (4) Tuteja, A.; Choi, W.; Ma, M. L.; Mabry, J. M.; Mazzella, S. A.; Rutledge, G. C.; McKinley, G. H.; Cohen, R. E. *Science* **2007**, *318*, 1618–1622.
- (5) Blossey, R. *Nat. Mater.* **2003**, *2*, 301–306.
- (6) Cao, L. L.; Jones, A. K.; Sikka, V. K.; Wu, J. Z.; Gao, D. *Langmuir* **2009**, *25*, 12444–12448.
- (7) Liu, K. S.; Jiang, L. *Nanoscale* **2011**, *3*, 825–838.
- (8) Nosonovsky, M.; Bhushan, B. *J. Phys.: Condens. Matter* **2008**, *20*.
- (9) Bico, J.; Marzolin, C.; Quere, D. *Europhys. Lett.* **1999**, *47*, 220–226.
- (10) Chen, W.; Fadeev, A. Y.; Hsieh, M. C.; Oner, D.; Youngblood, J.; McCarthy, T. J. *Langmuir* **1999**, *15*, 3395–3399.
- (11) Sun, T.; Wang, G. J.; Liu, H.; Feng, L.; Jiang, L.; Zhu, D. B. *J. Am. Chem. Soc.* **2003**, *125*, 14996–14997.
- (12) Brinker, C. J.; Scherer, G. W. *Sol–Gel Science: The Physics and Chemistry of Sol–Gel Processing*; Academic Press, Inc.: Boston, 1990.
- (13) Lannuzel, T. T. F.; Ameduri, B. M. F.; Guiot, J. P. S. C.; Boutevin, B. M. F. *Functionalized fluoromonomers and their copolymers with vinylidene fluoride*. U.S. Patent No. 0160,972, 2006.
- (14) Kabeta, K.; Zenbayashi, M.; Shinohara, K. Japanese Patent No. 3-17087-A, 1989.
- (15) Hirao, A.; Hayashi, M.; Loykulnant, S.; Sugiyama, K. *Prog. Polym. Sci.* **2005**, *30*, 111–182.
- (16) Templin, M.; Franck, A.; DuChesne, A.; Leist, H.; Zhang, Y. M.; Ulrich, R.; Schadler, V.; Wiesner, U. *Science* **1997**, *278*, 1795–1798.
- (17) Du, J. Z.; Chen, Y. M. *Angew. Chem., Int. Ed.* **2004**, *43*, 5084–5087.
- (18) Du, J. Z.; Chen, Y. M.; Zhang, Y. H.; Han, C. C.; Fischer, K.; Schmidt, M. *J. Am. Chem. Soc.* **2003**, *125*, 14710–14711.
- (19) Guo, A.; Liu, G. J.; Tao, J. *Macromolecules* **1996**, *29*, 2487–2493.
- (20) Ozaki, H.; Hirao, A.; Nakahama, S. *Macromolecules* **1992**, *25*, 1391–1395.
- (21) Sheen, Y. C.; Huang, Y. C.; Liao, C. S.; Chou, H. Y.; Chang, F. C. *J. Polym. Sci., Part B: Polym. Phys.* **2008**, *46*, 1984–1990.
- (22) Stober, W.; Fink, A.; Bohn, E. *J. Colloid Interface Sci.* **1968**, *26*, 62.
- (23) Liu, H. B.; Hamers, R. J. *Surf. Sci.* **1998**, *416*, 354–362.
- (24) Berne, B. J.; Pecora, R. *Dynamic Light Scattering with Applications to Chemistry, Biology, and Physics*; Dover Publications, Inc.: Mineola, NY, 1976.
- (25) DeLorenzi, L.; Fermeglia, M.; Torriano, G. *J. Chem. Eng. Data* **1996**, *41*, 1121–1125.
- (26) Ishizone, T.; Sugiyama, K.; Sakano, Y.; Mori, H.; Hirao, A.; Nakahama, S. *Polym. J.* **1999**, *31*, 983–988.
- (27) Pope, E. J. A.; Mackenzie, J. D. *J. Non-Cryst. Solids* **1986**, *87*, 185–198.

- (28) Kim, J.; Efimenko, K.; Genzer, J.; Carbonell, R. G. *Macromolecules* **2007**, *40*, 588–597.
- (29) Hirao, A.; Sugiyama, K.; Yokoyama, H. *Prog. Polym. Sci.* **2007**, *32*, 1393–1438.
- (30) Genzer, J.; Sivaniah, E.; Kramer, E. J.; Wang, J. G.; Korner, H.; Xiang, M. L.; Char, K.; Ober, C. K.; DeKoven, B. M.; Bubeck, R. A.; Chaudhury, M. K.; Sambasivan, S.; Fischer, D. A. *Macromolecules* **2000**, *33*, 1882–1887.
- (31) Furstner, R.; Barthlott, W.; Neinhuis, C.; Walzel, P. *Langmuir* **2005**, *21*, 956–961.
- (32) Cassie, A. B. D.; Baxter, S. *Trans. Faraday Soc.* **1944**, *40*, 0546–0550.
- (33) Wenzel, R. N. *Ind. Eng. Chem.* **1936**, *28*, 988–994.
- (34) Mugisawa, M.; Sawada, H. *Langmuir* **2008**, *24*, 9215–9218.
- (35) Visintin, P. M.; Carbonell, R. G.; Schauer, C. K.; DeSimone, J. M. *Langmuir* **2005**, *21*, 4816–4823.
- (36) Sawada, H.; Shikauchi, Y.; Kakehi, H.; Katoh, Y.; Miura, M. *Colloid Polym. Sci.* **2007**, *285*, 499–506.
- (37) Cui, X. J.; Zhong, S. L.; Yan, J.; Wang, C. L.; Zhang, H. T.; Wang, H. Y. *Colloids Surf., A* **2010**, *360*, 41–46.
- (38) Ofir, Y.; Samanta, B.; Arumugam, P.; Rotello, V. M. *Adv. Mater.* **2007**, *19*, 4075–79.
- (39) Wang, H. X.; Fang, J.; Cheng, T.; Ding, J.; Qu, L. T.; Dai, L. M.; Wang, X. G.; Lin, T. *Chem. Commun.* **2008**, 877–879.
- (40) Motornov, M.; Sheparovych, R.; Lupitskyy, R.; MacWilliams, E.; Minko, S. *Adv. Mater.* **2008**, *20*, 200–05.
- (41) Bravo, J.; Zhai, L.; Wu, Z. Z.; Cohen, R. E.; Rubner, M. F. *Langmuir* **2007**, *23*, 7293–7298.
- (42) Jasper, J. J. *J. Phys. Chem. Ref. Data* **1972**, *1*, 841.
- (43) Xiong, D. A.; Liu, G. J.; Zhang, J. G.; Duncan, S. *Chem. Mater.* **2011**, *23*, 2810–2820.